International Journal of Neural Systems, Vol. 21, No. 2 (2011) 139–149

DOI: 10.1142/S0129065711002729

World Scientific
www.worldscientific.com

TRANSCUTANEOUS FOCAL ELECTRICAL STIMULATION VIA CONCENTRIC RING ELECTRODES REDUCES SYNCHRONY INDUCED BY PENTYLENETETRAZOLE IN BETA AND GAMMA BANDS IN RATS

WALTER G. BESIO* and XIANG LIU†
Electrical, Computer, and Biomedical Engineering
University of Rhode Island, 4 East Alumni Ave.
Kingston, Rhode Island 02881,USA
**besio@ele.uri.edu*
†*liu@ele.uri.edu*

LILING WANG
2900 Kingstown Road, Kingston
Rhode Island 02881, USA
lwang@ele.uri.edu

ANDREI V. MEDVEDEV
Department of Neurology, Georgetown University
154 Building D, Washington, DC, USA
am236@georgetown.edu

KANTHAIAH KOKA
Department of Physiology and Biophysics
University of Colorado School of Medicine
Mail Stop 8307, P.O. Box 6511
12800 E 19th Ave, Aurora, Colorado 80045, USA
kanthu@gmail.com

Epilepsy is a neurological disorder that affects approximately one percent of the world population. Antiepileptic drugs are ineffective in 25∼30% of cases. Electrical stimulation to control seizures may be an additive therapy. We applied noninvasive transcutaneous focal electrical stimulation (TFES) via concentric ring electrodes on the scalp of rats after inducing seizures with pentylenetetrazole. We found a significant increase in synchrony within the beta-gamma bands during seizures and that TFES significantly reduced the synchrony of the beta-gamma activity and increased synchrony in the delta band.

Keywords: Epilepsy; electrical stimulation; seizure; synchrony; beta-gamma band; coherence.

1. Introduction

Epilepsy is a neurological disorder that affects approximately one percent of the world population with up to three-fourths of all patients with epilepsy in developing countries.[1] Over 50 million people worldwide are affected by epilepsy. Antiepileptic drugs used to treat epilepsy are ineffective in 25∼30% of cases and can cause side effects. Surgery is another option available, but carries risks. Aside from these solutions there are implantable electronic devices. Vagus nerve stimulation is FDA approved,[2] bilateral deep brain stimulation of the anterior nuclei of the thalamus (ANT)[3] and the responsive neurostimulator system (RNS)[4] are awaiting FDA approval.

In Theodore and Fisher's[5] review of brain stimulation techniques they concluded that the best

structures to stimulate and the most effective stimuli to use were still unknown. Previously Besio *et al.* showed that noninvasive transcutaneous focal electrical stimulation (TFES) via concentric ring electrodes attenuated the severity of behavioral and electrographic manifestations of status epilepticus induced by pilocarpine.[6] Pilocarpine is a strong convulsant and used as a rat model of status epilepticus because it causes recurrent and continual seizures when given in high concentrations (greater than 300 mg/kg).[7] Other reports mention administering antiepileptic drugs, such as diazepam, once every hour to keep seizures from recurring after pilocarpine-induced status epilepticus in rats.[8] We found that the normalization of electrographic activity was observed even two hours after the stimulation and beyond without administering any antiepileptic drugs such as diazepam. Thus, the observed sharp attenuation of pilocarpine-induced seizure activity after TFES was a promising finding suggesting a strong anti-convulsant mechanism engaged by TFES.

Mirski and Fisher have demonstrated a strong anticonvulsant effect of high frequency (100 Hz) electrical stimulation of the mammillary nuclei (MN) on pentylenetetrazol-induced seizures in rats.[9] They suggested that such stimulation had an inhibitory/desynchronizing effect on MN and thus destroyed synchronization between cortical-subcortical structures which appears to be necessary for generalized seizures to develop. Brain activity becomes more synchronized during the ictal state due to excessive excitation of neurons in the brain.[10] The synchronization spreads sporadically to different regions of the brain with highly nonlinear characteristics.[11] With the goal to clarify the mechanisms of anticonvulsant action of TFES which we previously observed in the rat pilocarpine model of epilepsy, we hypothesized that TFES could reduce the pathological synchronization of brain potentials especially at the early stages of seizure development. To test this hypothesis, in this study we applied TFES during seizures caused by pentylenetetrazole (PTZ) in rats. We used cross-channel coherence (CCC) to measure synchrony changes in electrographic activity recorded from the rat scalp. The CCC analysis allowed us to quantitatively evaluate the connectivity of regions of the brain under each electrode.

The CCC can be applied to signals recorded from any two electrodes and thus it measures linear correlation or interdependence of activities over time from two different regions of the brain. Cross-channel coherence is the frequency domain analog of the time domain correlation[12] and measures synchronization of EEG waves at particular frequencies.

Analysis was performed on three segments of electrographic activity for each rat namely, (1) before administration of the convulsant stage (referred to as Baseline), (2) after administration of the convulsant, PTZ, prior to TFES (referred to as Pre-TFES), and (3) the period immediately after TFES (referred to as Post-TFES). It was predicted that the Baseline period would show a relatively low inter-electrode coherence, the Pre-TFES stage would show a relatively high coherence, and the Post-TFES period would exhibit similar coherence as the Baseline stage if the TFES is effective.

2. Methods

Our animal protocol was approved by the University of Rhode Island IACUC. Approximately 24 hours before the induction of seizures, an adult male 220∼320 g Sprague-Dawley rat was given a combination of 80 mg/kg of ketamine and 12 mg/kg xylazine (i.p) for anesthesia. The scalp was shaved and prepared with NuPrep abrasive gel (D. O. Weaver & Co., Aurora, CO, U.S.A.). As depicted in Fig. 1, three custom-designed tripolar concentric ring electrodes[13] were applied to the scalp using conductive paste (0.5 mm Ten20, Grass Telefactor, RI, U.S.A.) and adhered with Teet's dental acrylic (Pearson Lab Supply, Sylmar, CA, U.S.A.).

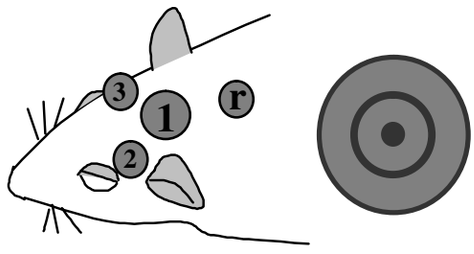

Fig. 1. The location of the tripolar concentric ring electrodes on the rat scalp. Electrode (1) is 10 mm dia. and used for stimulation and recording. Electrodes (2) and (3) are both 6.0 mm dia. and used only for recording. Electrode (r) is the reference. Details of a tripolar concentric ring electrode is shown to the right of the rat head.

One tripolar concentric ring electrode (1) (diameter = 10 mm with the width of each ring being 0.9 mm), used to record from and stimulate primarily the cerebral cortex, was centered on the top of the head. The front edge of the electrode was placed as close to the bregma as possible. Two other recording electrodes (2, 3) (diameter = 6 mm, ring width 0.4 mm) were placed bilaterally behind the eyes, but in front of the ears closer to the subcortical structures such as the hippocampus, thalamus, and midbrain than electrode (1). (A 2.0 mm, L 9.0 mm relative to the central electrode.) A reference electrode (r) was attached on the top of the neck behind the ears. These particular electrode locations were chosen due to size constraints and anatomy. The electrodes were made of gold-plated copper. Rats were returned to their cages and allowed food and water ad libitum for approximately 24 hours until the experimental procedure began. All experiments were performed in the afternoon.

On the following afternoon the rats were placed in a transparent plastic cage and the electrodes via a commutator and cables (Plastics One, Roanoke, VA,) were connected to a manual multiplexer. The multiplexer was first set to connect the electrodes to a Prep-Check Plus EIM-107 (General Devices, Ridgefield, N.J.) to measure skin-to-electrode impedance between each element of the three concentric ring electrodes and the reference electrode on the back of the neck. If the impedance for the outer ring and middle disc of electrode (b) of Fig. 1 was less than 10 KΩ the rat was a candidate for receiving TFES. If the outer ring or center disc skin-to-electrode impedance for the 1.0 cm dia. electrode (1) to the reference electrode (r) was greater than 10 KΩ, but less than 25 KΩ, the rat did not receive TFES and was put into the control group ($n = 3$) for recording only. The electrodes were then switched to the custom designed recording system. The EEG recording and the video were then started. After five minutes of baseline EEG recording the PTZ was administered (55 mg/kg, ip). At the end of the experiment the skin-to-electrode impedance was rechecked. To determine when to administer the TFES, the rat behavioral activity was closely monitored and scored for seizure-related phenomena according to a scheme adapted from Mirski *et al.*[14] The TFES (300 Hz, 50 mA, 200 μs, biphasic square pulses for 2 minutes) was administered immediately after the first myoclonic jerk was observed, which corresponded to a seizure activity level of Racine = 3. The control group rats did not receive TFES.

The EEG signals were preamplified (gain 100 and 0.3 Hz high pass filter) with a custom built preamplifier and then amplified using a Grass Model NRS2 Neurological Research System with Model 15A54 AC amplifiers (Grass Technologies, West Warwick, RI, USA) with a gain of 1,000 and band pass of 1.0–100 Hz with the 60 Hz notch filter active, and digitized (16 bits, 256 S/s). The digitized signals were stored on a computer hard drive for offline coherence analysis and display using Matlab. The two differential signals from each electrode were combined with an algorithm to give Laplacian derivation of the signal as reported previously by Besio.[13] Briefly, the algorithm is two-dimensional and weights the middle ring and disc difference sixteen times greater than the outer ring and disc difference.

Three thirty-second long artifact-free segments were processed for each experiment. In the TFES treated rats ($n = 6$) the Baseline segment was selected during the time period when the rats were relatively still for at least 30 seconds resulting in artifact free baseline EEG. The Pre-TFES and Post-TFES segments were always taken immediately before the TFES was turned on and just after the amplifiers recovered from the application of TFES, respectively. This particular Pre-TFES segment was selected since it should have had the electrographic activity that preceded the first R = 3 myoclonic jerk that was detected as the cue to turn the TFES on. The Post-TFES segment was chosen to be as soon after the amplifiers recover as possible before the rats started roaming and eating causing movement artifacts. For the control group we included similar segments; Baseline, the segment that corresponded to the Pre-TFES (immediately preceding the first R = 3 myoclonic jerk); and the segment 2.5 minutes after the first R = 3 myoclonic jerk (emulating the segment just after the application of TFES would have been stopped for a TFES-treated rat). Each 30 second segment (7,680 samples) was analyzed with a sliding 0.5 second window to calculate the CCC with a 128 point FFT. Figures were generated to show the EEG and the coherence between channels in relation to frequency and time. For Figs. 3, 4, and 6 the CCCs were smoothed with a five-point smoothing function

from Matlab (smooth with span set to 5) (Mathworks Natick MA, USA).

We used a custom in-house written Matlab program for data handling and the mscohere command to perform the CCC. The CCC utilized the power spectral density (Pxx and Pyy) of x and y and the cross power spectral density (Pxy) of x and y as in Eq. (1)

$$C_{xy}(f) = \frac{|P_{xy}(f)|^2}{P_{xx}(f)P_{yy}(f)}. \quad (1)$$

For statistical analysis a two-factor ANOVA was performed with 'electrode pairs' and 'temporal stage' (Baseline, Pre-TFES and Post-TFES) as factors performed on the CCC data using Matlab. The post hoc analysis was performed with the multcompare command in Matlab. The coherence values were compared over the following frequency bands: 1–4.5 Hz (delta), 5–8.5 Hz (theta), 9–13.5 Hz (alpha), 14–31.5 Hz (beta), 32–59.5 Hz (gamma).

We used single factor ANOVA with Bonferonni correction to test the effect of segment-length and TFES on the CCC. We analyzed the first 1, 2, 5, 10, 15, and 30 seconds of the Baseline, Pre-TFES, and Post-TFES segments.

3. Results

After five minutes of baseline recordings the PTZ was administered. Shortly after giving the PTZ, usually within two minutes, the rats had their first myoclonic jerk (Racine = 3). The time of the first myoclonic jerk was used as a cue to switch the electrodes to the custom in-house designed stimulator and turn it on to start TFES. Figure 2 shows the 30 second EEG recordings from the three electrodes of one rat that are indicative of the other data. In Fig. 2 the three temporal stages are Baseline (top row), Pre-TFES (middle row), and Post-TFES (bottom row). The PTZ-induced seizure activity accompanied by high voltage spikes and slow waves could be clearly seen during the Pre-TFES stage. In contrast, electrographic activity during the Baseline and Post-TFES stages was of much lower amplitude.

A pairwise cross correlation between all electrode signals was also performed on the same data segments from all TFES-treated rats with the correlation coefficients ranging from 0.08 to 0.71 with no significant difference between any of the segments. The CCC was used for the analysis since coherence gives information about specific frequency bands. Figure 3 shows the CCC between the three electrode pair combinations (top panel — electrodes 1 and 2, middle panel — electrodes 2 and 3, bottom panel — electrodes 1 and 3) for the signals shown in Fig. 2. In each of the electrode combinations the Pre-TFES CCC was consistently high over the full frequency range 1–50 Hz. The Baseline and Post-TFES CCC values were similar and lower than during the Pre-TFES stage. Figure 4 shows the CCC between the three electrode pairs for another rat. In this rat the same trends as shown in Fig. 3 were observed however the CCC was not as high during the Pre-TFES segment.

Figure 5 shows the grand average coherence averaged over six rats at five frequency bands. The electrode combinations are the same as in Fig. 3. It can be seen that the Pre-TFES stage shows a significantly higher coherence for all three electrode combinations in the beta ($p = 0.003^{**}$) and gamma ($p = 0.017^{*}$) bands compared to the other temporal stages. Figure 5 also shows that the coherence values within beta and gamma bands were very similar for the Baseline and Post-TFES stages. Figure 6 shows the CCC between the three electrodes for a control rat. We can see that the Baseline CCC was lower at all frequencies compared to other stages. After administration of the PTZ the CCC primarily increased at the higher frequencies. In contrast to the TFES-treated rats, the CCC from the segment 2.5 minutes after the first Racine = 3 myoclonic jerk continued to increase even further rather than trend towards the Baseline CCC.

Figure 7 shows the grand average coherence averaged over three control rats for the same five frequency bands. The electrode combinations are the same as for the other figures as well. It can be seen that 2.5 minutes after the first Racine = 3 myoclonic jerk, in all three electrode combinations, the coherence in the beta and gamma bands was higher than during the other temporal stages.

For the segment-length sensitivity analysis there was no significant difference (all p-values are shown in Table 1) between delta, theta, and alpha bands during Baseline, Pre-TFES, and Post-TFES stages for all segment-lengths tested. There was a significant decrease in CCC of beta and gamma bands after TFES for segement-lengths of 10 sec (also at

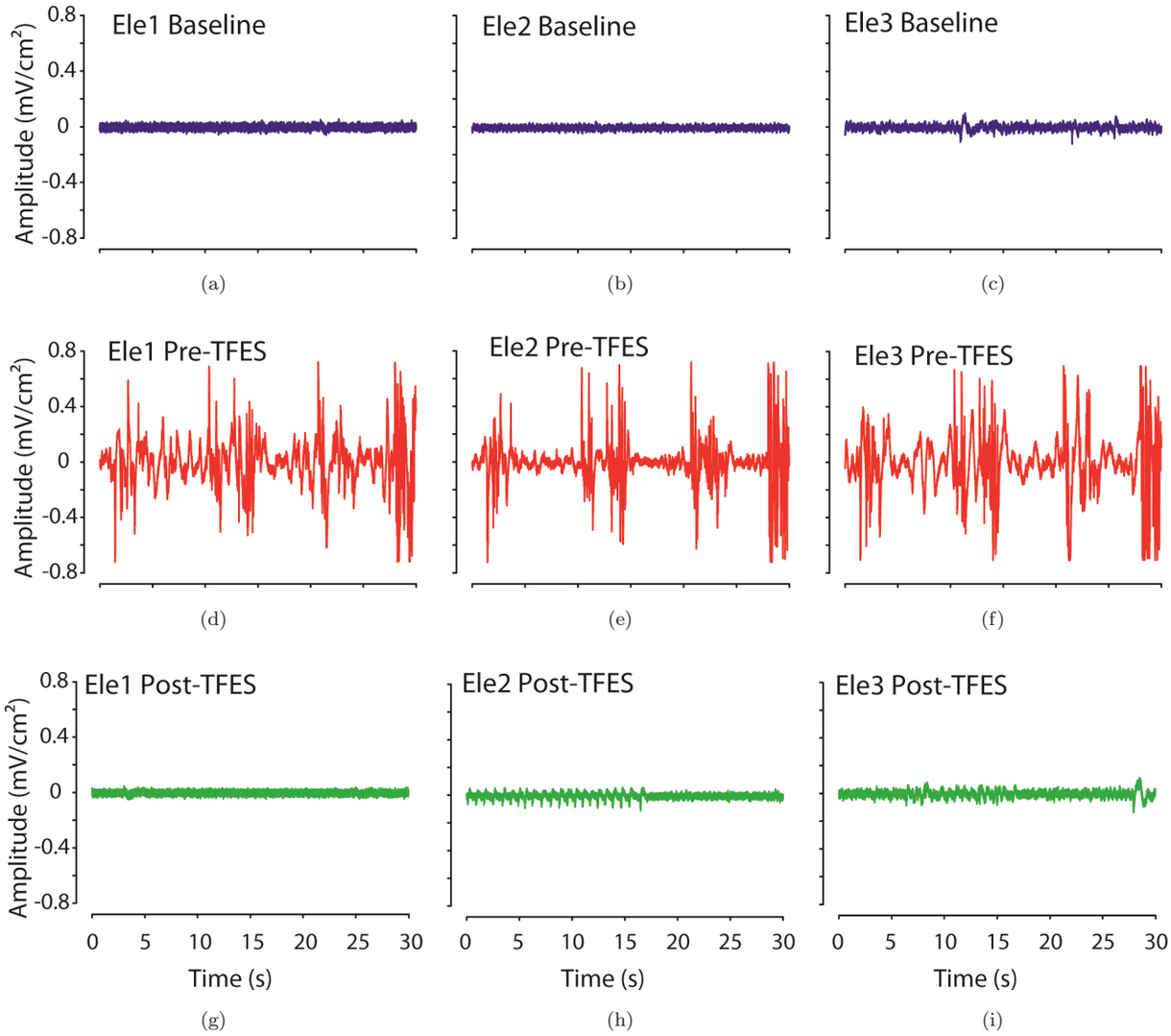

Fig. 2. Thirty second segments of Laplacian EEG recorded from each of the three electrodes during the three temporal stages. Ele1 – electrode 1, Ele2 – electrode 2, Ele3 – electrode 3, TFES – transcutaneous focal electrical stimulation via concentric ring electrode, Baseline – before administration of the PTZ, Pre-TFES – after administration of PTZ but prior to TFES, Post-TFES – after the amplifiers have recovered from TFES.

2 sec) or greater and no significant difference when 1 and 5 second segement-lengths were analyzed.

4. Discussion

The main finding of this work is that TFES significantly reduced the highly synchronized brain activity within the beta and gamma bands at the early stages of PTZ-induced seizure development. We also found that TFES increased the low-frequency synchrony in the delta band.

It is now apparent that in both humans and animal models of epilepsy high-frequency oscillations are present during seizures beyond the conventionally used 30 Hz upper bound for EEG recording.[15,16] There are several reports of increased cortical activity in the beta-gamma range observed in *in vitro* preparations that has been shown to result from synchronization of inhibitory GABAergic networks.[17,18] As stated earlier, seizure activity results in the abrupt outbursts of synchronized or correlated neurons. Synchronous activity in the brain can be

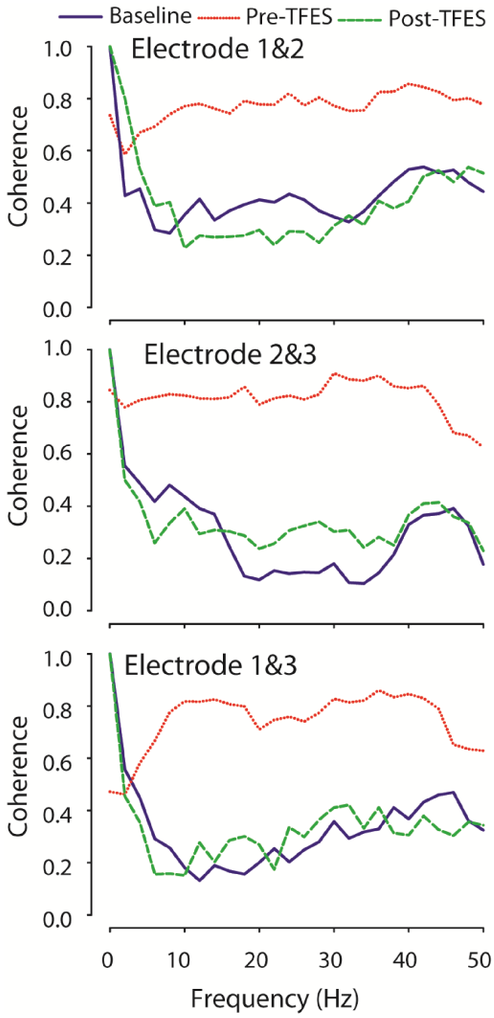

Fig. 3. Example #1 of smoothed CCC for TFES-treated rats – Top (electrodes 1 and 2), Middle (electrodes 2 and 3), Bottom (electrodes 1 and 3). The Pre-TFES CCC is high over a broad spectrum. The Baseline and Post-TFES are similar and less than the Pre-TFES CCC.

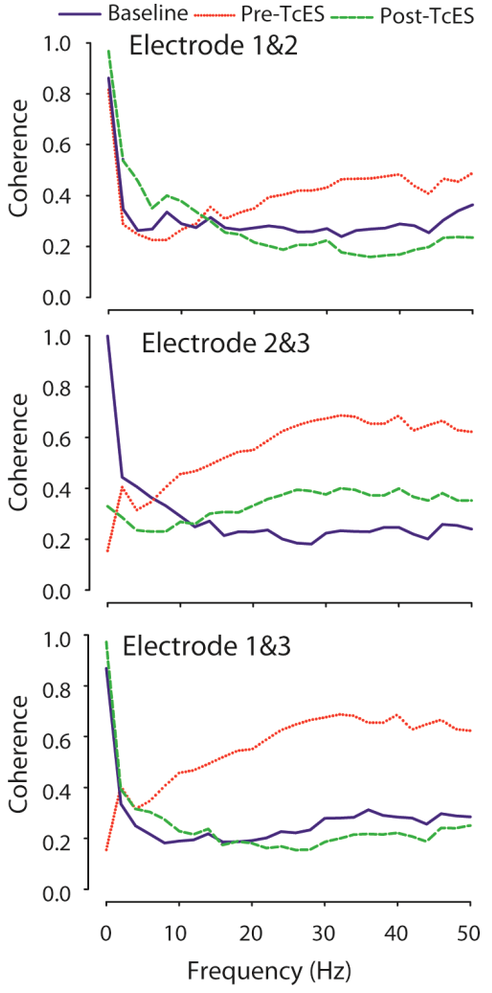

Fig. 4. Example #2 of smoothed CCC for TFES-treated rats – Top (electrodes 1 and 2), Middle (electrodes 2 and 3), Bottom – Top (electrodes 1 and 2), Middle (electrodes 2 and 3), Bottom (electrodes 1 and 3). The Pre-TFES CCC is high over a broad spectrum. The Baseline and Post-TFES are similar and less than the Pre-TfES CCC.

detected through coherence. In a review, Sitnikova[19] reported on increased coherence in the beta band during spike-wave discharges in thalamo-cortical and fronto-occipital regions of the rat brain. Blumenfeld *et al.*[20] found evidence for increased connectivity between the amygdala and frontal cortex both during seizures and in the interictal period, as a result of kindling. In a pilocarpine model, Tejada *et al.*[21] showed that the theta band coherence between the EEG signals recorded from the hippocampus and the frontal cortex increased after pilocarpine treatment but only during the waking states. Medvedev[22] showed that long before seizures induced by systemic application of kainic acid in rats, there was an increase in power and synchrony of gamma activity measured with intracortical recordings, probably due to excessive glutamatergic activation. During the initial stages of repetitive electrographic seizures (before the development of slow spike-wave rhythms), there was a further increase in gamma-band power and coherence (while during spike-wave rhythms the gamma-band coherence was reduced back to approximately baseline levels). Thus, epileptiform spikes and spike-wave rhythms were always preceded by outbursts

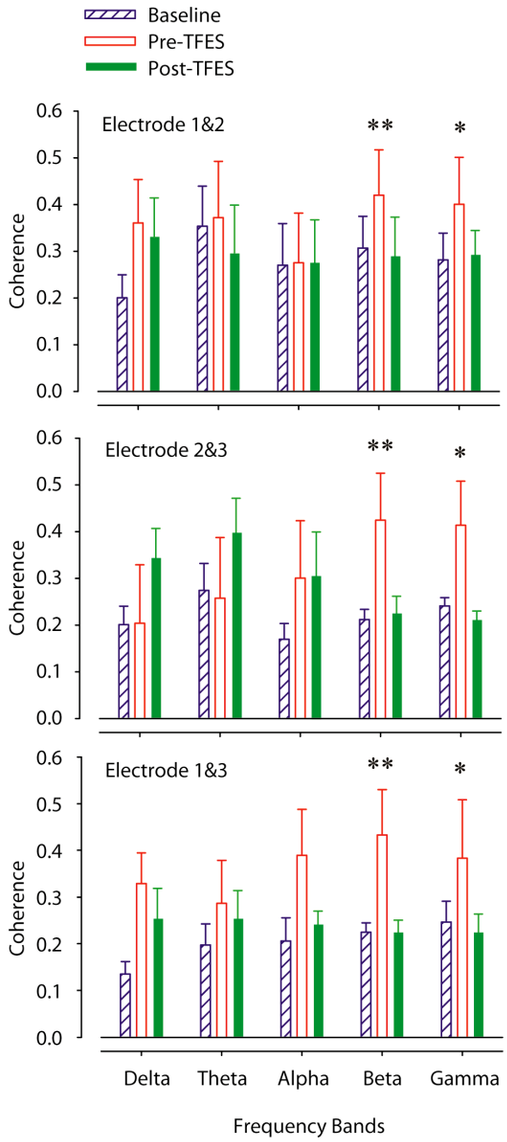

Fig. 5. Grand averaged CCC over all 6 rats at the different frequency bands analyzed – Top (electrodes 1 and 2), Middle (electrodes 2 and 3), Bottom (electrodes 1 and 3). There is a significant difference Post-TFES versus Pre-TFES at the $p = 0.05$ and 0.01 level for the beta and gamma bands (denoted by * and ** respectively). These are the bands at which TFES induced the most significant desynchronization with levels similar to the ones in the baseline.

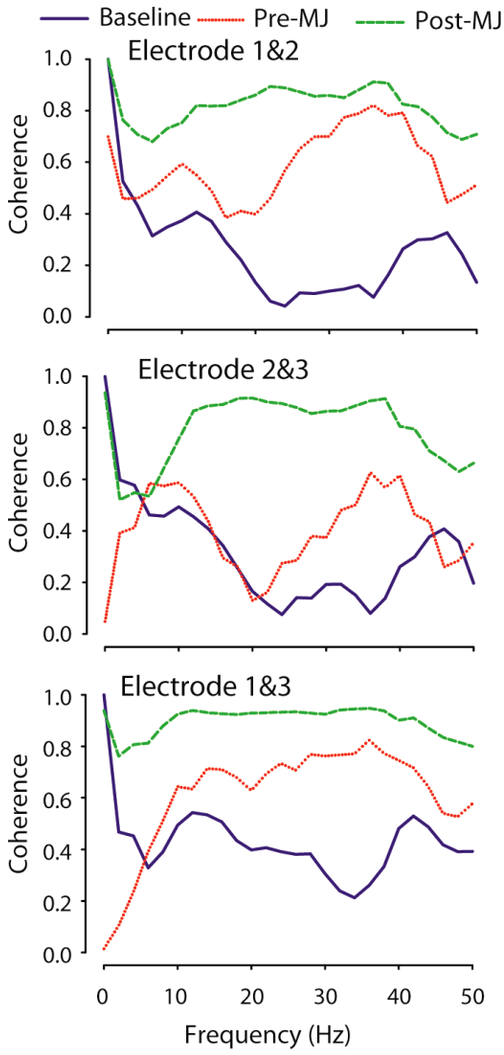

Fig. 6. The smoothed CCC for a control rat – Top (electrodes 1 and 2), Middle (electrodes 2 and 3), Bottom (electrodes 1 and 3). The Post-MJ CCC is highest over a broad spectrum. The Pre-MJ is higher than the Baseline CCC. Pre-MJ, 30 second segment immediately preceding the first R = 3 myoclonic jerk, emulating the segment just before the TFES was turned on in the TFES-treated rats. Post-MJ, the 30 second segment beginning 2.5 minutes after the first R = 3 myoclonic jerk, emulating the segment just after the application of TFES would have been stopped for a TFES-treated rat.

of gamma-band activity while the reverse was not true (spikes did not immediately precede increased gamma activity). Lévesque *et al.* also showed that gamma oscillations in the amygdalo-hippocampal network could facilitate long-range synchrony and participate in the propagation of seizures.[23]

Our preliminary results are in line with the above reports. We also found a significant increase in synchrony in the frontal regions of the brain. However, it should be noted that these previous reports were made using implanted electrodes or slice recordings. In contrast, we measured

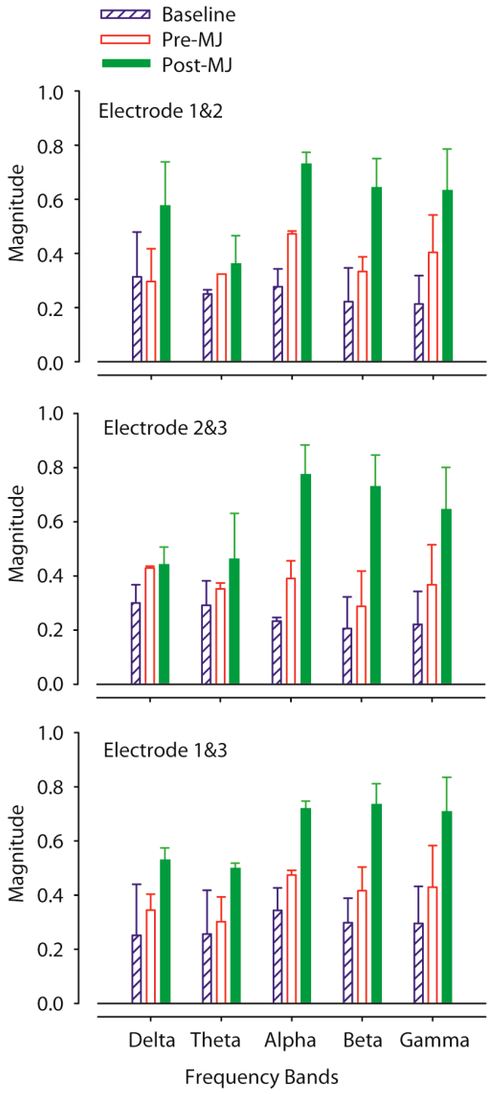

Fig. 7. Grand averaged CCC over all 3 control rats at the difference frequency bands analyzed – Top (electrodes 1 and 2), Middle (electrodes 2 and 3), Bottom (electrodes 1 and 3). The Post-MJ CCC is highest over a broad spectrum. The Pre-MJ is higher than the Baseline CCC.

coherence changes from the scalp surface, where the skull and the scalp sharply attenuate high-frequency oscillations, and are not typically present in recordings made with conventional disk electrodes. As Besio *et al.* reported previously, concentric ring electrodes provide significant improvement in spatial resolution (4 times), mutual information (10 times), and signal-to-noise ratios (4 times) than conventional disc electrodes.[13] Due to these improvements,

Table 1. Statistical parameters from Bonferroni corrected ANOVA test.

	Delta	Theta	Alpha	Beta	Gamma
1 sec	0.587	0.152	0.881	0.090	0.114
2 sec	0.278	0.529	0.490	**0.030**	**0.014**
5 sec	0.044	0.749	0.969	0.256	0.228
10 sec	0.203	0.295	0.400	**0.003**	**0.002**
15 sec	0.298	0.802	0.726	**0.013**	**0.031**
30 sec	0.059	0.839	0.297	**0.002**	**0.011**

concentric ring electrodes are less sensitive to the spatial smearing of neural signals by scalp and therefore measure a much more localized signal from the specific areas of the brain directly below them. As a result, we were able to reliably detect the beta and gamma band activity from the scalp surface.

Medvedev[24] proposed that ictogenesis starts with hypersynchrony of high-frequency oscillations due to a pathological process and that there should be an 'emergency mechanism' in the brain to shut them down when the hypothetical inhibitory mechanisms controlling gamma rhythms become insufficient. Although seizures can be devastating, Medvedev suggested this may be the brain's protective mechanism preventing, or at least diminishing, severe cognitive impairments which otherwise would be likely because of the excessive 'temporal binding' at high frequencies. The spike and spike-slow wave activity known to be a hallmark of epilepsy is in the 2 to 4 Hz range and was suggested to represent a synchronizing event different from the hypersynchrony at high frequencies.[22,24] Based on slice and modeling studies, Traub *et al.*[25] have emphasized a quantitative difference between synchrony at high frequencies and synchrony of epileptiform events. Gamma oscillations are usually synchronized with phase delays of a few milliseconds at distances over 4 mm (for review, see Traub *et al.*,[26] also Medvedev.[22]) On the other hand, epileptic activity on this spatial scale is synchronized with delays of around 20 ms.[25] Based on these observations, Medvedev has suggested that a less precise but massive synchronization at low frequencies during spike-wave rhythms is likely to destroy precise synchronization and fine temporal structure of high frequency rhythms.[24] The suggested antagonistic nature of gamma-band rhythms and spike-wave activity has been proposed by Medvedev for the protective role of seizures

diminishing pathologically increased gamma-band synchrony.[24] In conceptual proximity to this idea of a protective role of seizures, Iasemidis, Sackellares and colleagues described disentrainment of the EEG dynamics within neural systems caused by ictal activity and suggested that this seizure-related disentrainment could play a 'resetting' role.[27–30]

It could be proposed that the TFES, which reduced synchrony of the beta and gamma activity and caused a transient period of increased synchrony at delta frequencies, caused a reorganization of neural dynamics somewhat similar to that caused by seizures. Thus, the TFES effect was 'simulating' a seizure but, we hope, without the detrimental aspects of the seizure. Therefore, a possible interpretation of the seizure-aborting capability of the TFES is that the seizure was no longer necessary for protecting the brain from the hypersynchronized beta-gamma activity.

Comparing the control rats to the TFES-treated rats, we can see a stark contrast in coherence values. For the single control rat (Fig. 6) during the segment starting 2.5 minutes after the first myoclonic jerk (Post-MJ), corresponding to the Post-TFES segment in the TFES-treated rats, the CCC was higher than for the other segments suggesting that the synchrony has continued to increase over time. In contrast, in TFES-treated rats, the Post-TFES coherence was similar to the Baseline coherence suggesting that TFES lowered the synchrony previously induced by PTZ. A similar contrast can be observed comparing the grand averages between the controls (Fig. 7) and TFES-treated rats (Fig. 5).

Our sensitivity analysis showed that 10-second segments or longer were necessary for the statistical significance of the coherence to be stable. There was a significant difference between groups and conditions when calculating CCC using 2-second segments. However, when we increased the segment length to 5 seconds there was no significant difference in the CCC for the Baseline, Pre-TFES, and Post-TFES segments. This could be due to a waxing and waning period of seizure activity in the early stages after administration of the PTZ.

Based on the current finding that TFES significantly reduced PTZ-induced hypersynchrony at the beta and gamma frequencies, as well as our previous reports of reduction of the effects of pilocarpine-induced[6] status epilepticus and severe penicillin-induced[31] myoclonic jerks, we suggest that TFES may have anticonvulsant effects, at least in rats. For future work we propose to test different stimulation parameters for optimal efficacy of the TFES. It would also be of interest to couple TFES and signals from tripolar concentric ring electrodes with various seizure prediction and detection algorithms.[32–43]

It should also be noted that there have been concerns raised about using coherence to measure synchrony of various areas of the brain.[44–45] In particular the use of a quiet reference is needed for accurate coherence calculations.[44–46] Nunez suggested using a global spline-Laplacian, the second spatial derivative of the scalp potentials, to overcome the reference problem.[46] We have shown previously that the Laplacian-transformed potentials recorded from our tripolar concentric ring electrode have significantly less mutual information than conventional EEG.[47] This leads us to believe that the tripolar concentric ring electrode isolates signals from sources that are more independent than conventional EEG. Therefore, the tripolar concentric ring electrode and our custom instrumentation help alleviate the concerns raised for scalp-recorded coherence as a measure of synchronous brain activity.

Acknowledgments

WGB would like to thank Ahmad Paintdakhi for his help analyzing data for a previous version of this manuscript and Dr. Oleksandr Makeyev for our discussions on sensitivity. We would also like to thank the staff at the URI Central Lab Animal Facility for their help with animal handling. The project described was supported in part by Award Number R21NS061335 from the National Institute of Neurological Disorders and Stroke. The content is solely the responsibility of the authors and does not necessarily represent the official views of the National Institute of Neurological Disorders and Stroke or the National Institutes of Health. It was also supported in part by a grant from the Rhode Island Foundation.

References

1. J. W. Sander, The epidemiology of epilepsy revisited, *Curr. Oppin. Neurol.* **16**(2) (2003) 165–170.
2. R. Fisher and A. Handforth, Reassessment: Vagus nerve stimulation for epilepsy: A report of the

Therapeutics and Technology Assessment subcommittee of the american academy of neurology, *Neurology* **53**(4) (1999) 666–669.
3. R. Fisher and the SANTE Study Group, Electrical stimulation of the anterior nucleus of thalamus for treatment of refractory epilepsy, *Epilepsia* **51**(5) (2010) 899–908.
4. M. J. Morrell and the RNS System Pivotal Investigators, Results of a multicenter double blinded randomized controlled pivotal investigation of the RNS^{TM} system for treatment of intractable partial epilepsy in adults, American Epilepsy Society Conference abstract (2009) 1.102.
5. W. Theodore and R. Fisher, Brain stimulation for epilepsy, The *Lancet* **3**(2) (2004) 111–118.
6. W. Besio, K. Koka and A. Cole, Feasibility of noninvasive transcutaneous electrical stimulation for modulating pilocarpine-induced status epilepticus seizures in rats, *Epilepsia* **48**(12) (2007) 2273–2279.
7. W. A. Turski, E. A. Cavalheiro, M. Schwarz, S. J. Czuczwar, Z. Kleinrok and L. Turski, Limbic seizures produced by pilocarpine in rats: Behavioural, electroencephalographic and neuropathological study. *Behav. Brain Res.* **9**(3) (1983) 315–335.
8. H. Goodkin, X. Liu and G. Holmes, Diazepam terminates brief but not prolonged seizures in young, naive rats, *Epilepsia* **44** (2003) 1109–1112.
9. M. A. Mirski and R. S. Fisher, Electrical stimulation of the mammillary nuclei increases seizure threshold to pentylenetetrazol in rats, *Epilepsia* **35**(6) (1994) 1309–1316.
10. L. D. Iasemidis, D. S. Shaiau, J. C. Sackellares, P. M. Pardalos and A. Prasad, Dynamical resetting of the human brain at epileptic seizures: Application of nonlinear dynamics and global optimization techniques, *IEEE Trans. BME* **51**(3) (2004) 493–506.
11. X. Li and G. Ouyang, Nonlinear similarity analysis for epileptic seizures prediction, *Nonlinear Analysis, Theory, Methods and Applications* **64**(8) (2006) 1666–1678.
12. S. Chillemi, R. Balocchi, A. Di Garbo, C. E. Dattellis, S. Gigola and S. Kochen, Discriminating preictal from interictal states by using coherence measures, *Proc of the 26th Conf. IEEE EMB Conf.* **3** (2003) 2319–2322.
13. W. Besio, K. Koka, R. Aakula and W. Dai, Tri-polar concentric ring electrode development for Laplacian electroencephalography, *IEEE Trans BME* **53**(5) (2006) 926–933.
14. M. Mirski, L. Rossell, J. Terry and R. Fisher, Anticonvulsant effect of anterior thalamic high frequency electrical stimulation in the rat, *Epilepsy Research* **28** (1997) 89–100.
15. G. A. Worrell, L. Parish, S. D. Cranstoun, R. Jonas, G. Baltuch and B. Litt, High-frequency oscillations and seizure generation in neocortical epilepsy, *Brain* **127** (2008) 1496–1506.
16. M. de Curtis and V. Gnatkovsky, Reevaluating the mechanisms of focal inctogenesis the role of low-voltage fast activity, *Epilepsia* **50**(12) (2009) 2514–2525.
17. M. A. Whittington and R. D. Traub, Interneuron Diversity Series: Inhibitory interneurons and network oscillations in vitro, *Trends in Neurosciences* **26**(12) (2003) 667–682.
18. R. D. Traub, M. O. Cunningham, T. Gloveli, F. E. N. LeBeau, A. Bibbig, E. H. Buhl and M. A. Whittington, GABA-enhanced collective behavior in neuronal axons underlies persistent gamma-frequency oscillations, *PNAS* **100**(19) (2003) 11047–11052.
19. E. Sitnikova, Thalamo-cortical mechanisms of sleep spindles and spike — Wave discharges in rat model of absence epilepsy (a review), *Epilepsy Res.* **89**(1) (2010) 17–26.
20. H. Blumenfeld, M. Rivera, J. G. Vasquez, A. Shah, D. Ismail, M. Enev and H. P. Zaveri, Neocortical and Thalamic Spread of Amygdala Kindled Seizures, *Epilepsia* **48**(2) (2007) 254–262.
21. S. Tejada, J. J. González, R. V. Rial, A. M. L. Coenen, A. Gamundí and S. Esteban, Electroencephalogram functional connectivity between rat hippocampus and cortex after pilocarpine treatment, *Neuroscience* **165** (2010) 621–631.
22. A. V. Medvedev, Epileptiform spikes desynchronize and diminish fast (gamma) activity of the brain: An "anti-binding" mechanism? *Brain Research Bulletin* **58**(1) (2002) 115–128.
23. M. Lévesque, J. M. P. Langlois, P. Lema, R. Courtemanche, G. A. Bilodeau and L. Carmant, Synchronized gamma oscillations (30–50 Hz) in the amygdalo-hippocampal network in relation with seizure propagation and severity, *Neurobiology of Disease* **35** (2009) 209–218.
24. A. V. Medvedev, Temporal binding at gamma frequencies in the brain: Paving the way to epilepsy? *Australasian Physical & Engineering Sciences in Medicine* **24**(1) (2001) 37–48.
25. R. D. Traub, J. G. Jefferys and M. A. Whittington, Functionally relevant and functionally disruptive (epileptic) synchronized oscillations in brain slices, *Adv. Neurol.* **79** (1999b) 709–724.
26. R. D. Traub, J. G. Jefferys and M. A. Whittington, Fast oscillations in cortical circuits, Cambridge, MA: MIT Press; (1999a).
27. J. C. Sackellares, L. D. Iasemidis, R. L. Gilmore and S. N. Roper, Epileptic seizures as neural resetting mechanisms, *Epilepsia* **38**(S3) (1997) 189.
28. D. S. Shiau, Q. Luo, R. L. Gilmore, S. N. Roper, P. Pardalos, J. C. Sackellares and L. D. Iasemidis, Epileptic seizures resetting revisited, *Epilepsia* **41**(S7) (2000) 208–209.

29. L. D. Iasemidis, D. S. Shiau, J. C. Sackellares, P. M. Pardalos and A. Prasad, Dynamical resetting of the human brain at epileptic seizures: Application of nonlinear dynamics and global optimization techniques, *IEEE Trans BME* **51** (2004) 493–506.
30. S. Sabesan, N. Chakravarthy, K. Tsakalis, P. Pardalos and L. D. Iasemidis, Measuring resetting of brain dynamics at epileptic seizures: Application of global optimization and spatial synchronization techniques, *J. Combinatorial Optimization* **17** (2009) 74–97.
31. W. G. Besio, K. Koka, K. S. Gale and A. V. Medvedev, Preliminary data on anticonvulsant efficacy of transcutaneous electrical stimulation via novel concentric ring electrodes, in S. C. Schachter, J. V. Guttag, S. J. Schiff, D. L. Schomer (summit contributors), Advances in the application of technology to epilepsy: The CIMIT/NIO Epilepsy Innovation Summit, Boston, May 2008, *Epilepsy Behav.* **16**(1) (2009) 3–46.
32. L. D. Iasemidis, Epileptic seizure prediction and control, *IEEE Trans. BME* **50**(5) (2003) 549–558.
33. K. Lehnertz, F. Mormann, H. Osterhage, A. Muller, J. Prusseit, A. Chernihovskyi, M. Staniek, D. Krug, S. Bialonski and C. E. Elger, State-of-the-art of seizure prediction, *Journal of Clinical Neurophysiology* **24**(2) (2007) 147–153.
34. J. C. Sackellares, Seizure prediction, *Epilepsy Currents* **8**(3) (2008) 55–59.
35. L. D. Iasemidis, S. Sabesan, L. Good, N. Chakravarthy, D. M. Treiman, J. Sirven, and K. Tsakalis, A new look into epilepsy as a dynamical disorder: Seizure prediction, resetting and control, in Philip Schwartzkroin, (ed.), *Encyclopedia of Basic Epilepsy Research* **3** (2009) 1295–1302. Elsevier.
36. K. Tsakalis and L. D. Iasemidis, Control aspects of a theoretical model for epileptic seizures, *Int. Journal of Bifurcations and Chaos* **16** (2006) 2013–2027.
37. N. Chakravarthy, S. Sabesan, L. D. Iasemidis and K. Tsakalis, Modeling and controlling synchronization in a neuron-level population model, *Int. J. Neural Systems* **17** (2007) 123–138.
38. N. Chakravarthy, K. Tsakalis, S. Sabesan and L. D. Iasemidis, Homeostasis of brain dynamics in epilepsy: A feedback control systems perspective of seizures, *Annals of BME* **37**(3) (2009) 565–585.
39. L. Good, S. Sabesan, S. Marsh, K. Tsakalis, D. Treiman and L. D. Iasemidis, Control of synchronization of brain dynamics leads to control of epileptic seizures in rodents, *Int. J. Neural Systems* **19**(3) (2009) 173–196.
40. M. P. Jacobs, G. D. Fischbach, M. R. Davis, M. A. Dichter, R. Dingledine, D. H. Lowenstein, M. J. Morrell, J. L. Noebels, M. A. Rogawski, S. S. Spencer and W. H. Theodore, Future directions for epilepsy research, *Neurology* **57**(9) (2001) 1536–1542.
41. B. Litt and K. Lehnertz, Seizure prediction and the preseizure period, *Curr Opin Neurol* **15**(2) (2002) 173–177.
42. O. Faust, U. R. Acharya, L. C. Min and B. H. C. Sputh, Automatic identification of epileptic and background EEG signals using frequency domain parameters, *International Journal of Neural Systems* **20**(2) (2010) 159–176.
43. H. Adeli, S. Ghosh-Dastidar and N. Dadmehr, A wavelet-chaos methodology for analysis of EEGs and EEG sub-bands to detect seizure and epilepsy, *IEEE Trans BME* **54**(2) (2007) 205–211.
44. R. Guevara, J. L. Velazquez, V. Nenadovic, R. Wennberg, G. Senjanovic and L. G. Dominguez, Phase synchronization measurements using electroencephalographic recordings: What can we really say about neuronal synchrony? *Neuroinformatics* **3**(4) (2005) 301–314.
45. S. J. Schiff, Dangerous phase, *Neuroinformatics* **3**(4) (2005) 315–318.
46. P. L. Nunez, R. B. Silberstein, P. J. Cadiush, J. Wijesinghe, A. F. Westdorp and R. Srinivasan, A theoretical and experimental study of high resolution EEG based on surface laplacians and cortical imaging, *EEG Clin. Neurophysiol.* **90** (1994) 40–57.
47. K. Koka and W. Besio, Improvement of spatial selectivity and decrease of mutual information of tri-polar concentric ring electrodes, *J of Neuroscience Methods* **165** (2007) 216–222.